

# Development and construction of COMBAT: a multi-planar silicon pixel tracker

**Vinicius Franco Lima<sup>1</sup>, Kazuyoshi Akiba<sup>1</sup>, Érica Polycarpo<sup>1</sup>**

<sup>1</sup> Instituto de Física, Universidade Federal do Rio de Janeiro;

E-mail: [viniciuslima@if.ufrj.br](mailto:viniciuslima@if.ufrj.br)

**Abstract:** In the present article the design of COMBAT (COMpactBrAzilian Telescope) a reduced radiation length tracking apparatus is discussed, along with a preliminary analysis on a 4 detector plane prototype measuring atmospheric muons.

**Keywords:** Telescope, Tracking, Timepix, High Resolution.

## 1. INTRODUÇÃO

In High Energy Physics (HEP), telescopes are systems built for the test of devices under development in a test-beam environment, where well controlled sources of high momentum particles can be used in conditions similar to those observed in actual experiments. They are usually composed of several planes of detectors providing 2-dimensional position, from which 3-dimensional trajectories can be reconstructed.

In this article we show the design of COMBAT, a lightweight setup and low material silicon planar telescope conceived for the test of pixel detectors for the LHCb experiment [1] at CERN. We also present preliminary results obtained with a first prototype illuminated by cosmic muons.

Each one of the COMBAT detector planes is composed of a Timepix front-end chip and 150 silicon (Si) sensors. These sensors have a  $1.98 \text{ cm}^2$  sensitive area divided into 65536 pixels of  $55 \text{ }\mu\text{m}$  pitch, which are read out in parallel.

## 2. COMBAT DESIGN

The COMBAT concept is of a portable system that can be operated in different test beam facilities with charged particle beams, such as  $e^\pm$ ,  $p^\pm$ ,  $\pi^\pm$ ,  $\mu^\pm$ , at different energies, still maintaining excellent spatial resolution. These requirements lead to the use of a light and stable mechanical structure with quick assembly capability, achieved with commercial aluminum rails and breadboards (figure 1).

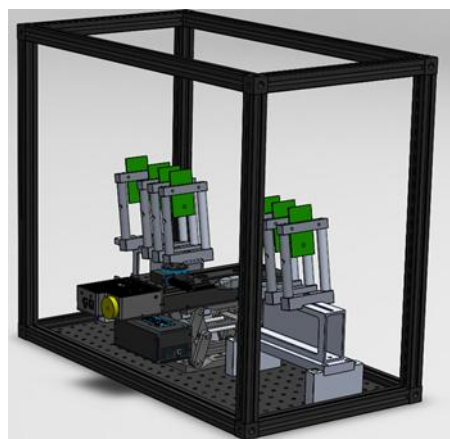


Figure 1: COMBAT graphic design.

The performance of position sensitive devices can only be studied with particle trajectories determined with precision higher than their own

spatial resolution. The precision of trajectories reconstructed with telescopes improves with the number of detector layers and the spatial resolution of the detectors, but degrades with the amount of material in each layer.

The spread in scattering angle due to multiple Coulomb scattering of a charged particle passing through a material is described by equation (1),

$$\theta_{rms} = \frac{13.6 MeV}{\beta c p} z \sqrt{x/X_0} [1 + 0.038 \ln \left( \frac{x}{X_0} \right)] \quad (1)$$

where  $\beta c$  and  $p$  are the incident particle's velocity and momentum, respectively,  $z$  is its charge and  $x/X_0$  is the amount of traversed material in units of the radiation length [3].

Multiple scattering thus limits the track resolution and may hinder the telescope performance, especially when operating with electrons. The angular spread for a 4 GeV electron beam scattered by the available Timepix assemblies are given in table 1. These angular spreads translate into the position spreads  $\sigma_{x,y}$  also given in table 1. Table 1 shows that spatial resolutions due to multiple scattering are smaller than the intrinsic precision of the Timepix detectors only for assemblies 2 and 4. Due to the availability of these assemblies in the next couple of years, the baseline COMBAT design consists of 4 planes using assembly 2 and 4 planes using assembly 4, which are composed of 150  $\mu m$  thick sensors and 750 and 100  $\mu m$  thick Timepix chips, respectively.

Table 1: Assembly possibilities and respective angular spreads, with resolutions calculated at 5 cm distance from plane, due to multiple scattering of a 4 GeV Electron beam.

	$x/X_0$ (%)	$\Theta_{rms}$ (mrad)	$\sigma_{x,y}$ ( $\mu m$ )
Assembly 1	2.06	0.42	20.80
Assembly 2	0.96	0.27	13.71
Assembly 3	1.47	0.35	17.32
Assembly 4	0.37	0.16	8.18

### 3. TIMEPIX AND READOUT SYSTEM

#### 3.1. Timepix

The Timepix is a CMOS front-end chip connected directly to the bottom of the sensor through a bump bonding process, in a way that each sensor pixel is connected to a front-end channel[4]. Signals are acquired within a controllable time window, called from now on a *frame*. In the end of the frame, the whole 256x256 pixel matrix is readout.

The readout can be done in 3 different modes: Time over Threshold (ToT), Time of Arrival (ToA) and counting mode. The ToT mode provides a digital response proportional to the energy deposited in the sensor (by measuring the time an incoming signal stays above threshold). The ToA mode provides the time the signal crosses a threshold with respect to a global time, with resolution up to 25 ns. In the counting mode the output is the number of hits per frame.

The telescope can be operated with a combination of planes in ToA and ToT modes, or with all planes working in the same mode. The ToT mode allows the determination of the position by the use of the charge centroid method with resolution better than the intrinsic geometric resolution. In ToA mode, hits in different planes can be selected according to the ToA, improving the performance of the tracking finding algorithm. Each readout channel has an independent tunable threshold, which allows operation in a “noise-free” mode.

#### 3.2. Readout System

Four planes can be readout simultaneously using the RelaxD readout system [6], with rates up to 1 MHz. The data output is done through a 1Gb connection using TCP/IP protocol. All configuration and data taking are managed by the Pixelman software [5].

#### 4. DETECTOR CALIBRATION

In order to have a direct comparison among the energy deposition spectra in the 4 telescope planes, an  $\text{Am}^{241}$  source is used to calibrate the ToT of the detectors. The ToT spectrum of the  $\text{Am}^{241}$  in all planes is shown in figure 2. A Gaussian curve is used to fit the peaks corresponding to the energies of the 11.0, 17.8, 26.0 and 59.5 keV photons.

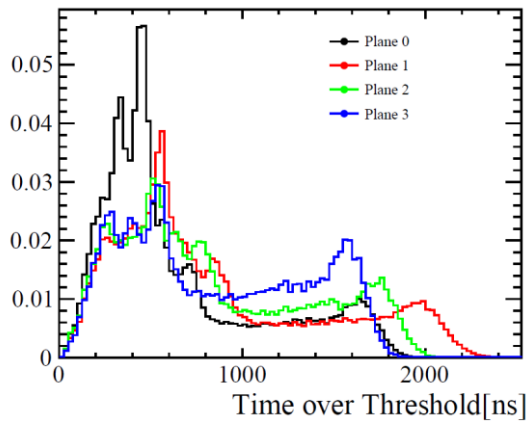


Figure 2: ToT spectrum for all detector planes.

Assuming a linear dependence of the ToT with the energy, the calibration curves for the four planes seen in figure 3 are obtained. The fitted calibration parameters are shown in table 2.

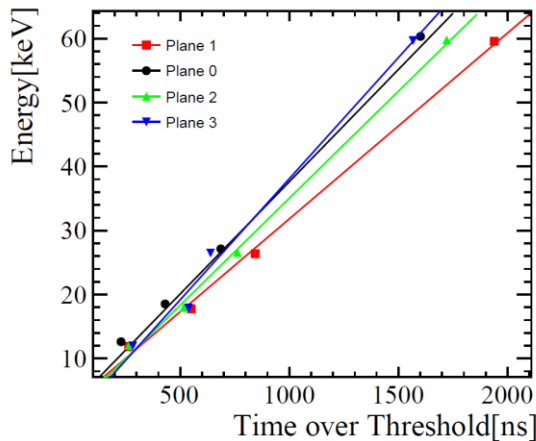


Figure 3: Calibration curves for all 4 planes.

Table 2: Fitted calibration parameters for all planes.

	Slope[leV/ns]	Intercept[keV]
Plane 0	$0.035 \pm 0.001$	$2.54 \pm 0.76$
Plane 1	$0.029 \pm 0.001$	$2.76 \pm 1.23$
Plane 2	$0.033 \pm 0.001$	$1.59 \pm 1.20$
Plane 3	$0.038 \pm 0.002$	$0.24 \pm 2.30$

#### 5. RESULTS

The results presented in this section are obtained with the prototype telescope and a dataset corresponding to  $6.4 \times 10^6$  frames of 100ms each. Out of the 6 million frames, only 196 have signals in all 4 planes. These 196 frames are the input for the track finding algorithm.

##### 5.1 Track Reconstruction

In each plane, neighbor hits are organized in clusters and the  $x$  position of the cluster is calculated as the centre-of-gravity of the pixel coordinates, using the ToT from the individual pixels as weighting factors.

For each frame, all possible combinations of clusters in the four planes are fitted to a straight line in 3 dimensions, using the least-squares method. The  $z$  position is of each plane if fixed to its measured value, assuming the detectors are perfectly horizontal and thus all pixels from the same plane have the same  $z$  position.

Having the parameters for all tracks traversing the telescope, we can calculate the residual distributions, i.e. the difference between the measured cluster position and the fitted track at each plane. Figure 4a shows that these distributions are not centered at zero, as one would expect for perfectly aligned sensors. We correct for this effect by refitting all tracks with the cluster positions subtracted from the mean values of the Gaussian functions fitted to the correction, the new residual distributions are all centered in zero, as shown in figure 4b. The

behavior of the residual in the  $y$  direction is similar. The width  $\sigma$  of a Gaussian fit to the final residual distribution is interpreted as the resolution of the telescope. The  $x$  and  $y$  resolutions computed with such fits are shown in table 3.

Table 3: Resolution results for aligned planes

	$\sigma_x$ [ $\mu\text{m}$ ]	$\sigma_y$ [ $\mu\text{m}$ ]
Plane 0	$20.6 \pm 1.6$	$22.0 \pm 1.7$
Plane 1	$31.7 \pm 4.3$	$33.0 \pm 2.7$
Plane 2	$43.7 \pm 4.9$	$43.7 \pm 4.9$
Plane 3	$25.5 \pm 2.1$	$25.4 \pm 2.3$

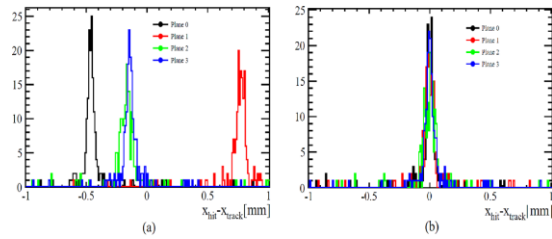


Figure 4: Residual distribution in each plane, before (a) and after (b) alignment.

Excluding tracks with a  $\chi^2$  probability less than 98%, to reject fake tracks, we conclude that a total of  $166 \pm 12$  particles traversed the telescope, compared with the 155 expected by convoluting the atmospheric muon rate [2] with the geometric acceptance of the telescope.

With the detectors calibrated, the energy deposited in the sensors by the reconstructed cosmic rays can be measured, as shown in figure 4. The most probable energy deposit is compatible among the four planes and with the energy expected to be deposited by a MIP in 150  $\mu\text{m}$  silicon sensor, of 39.6 keV[3].

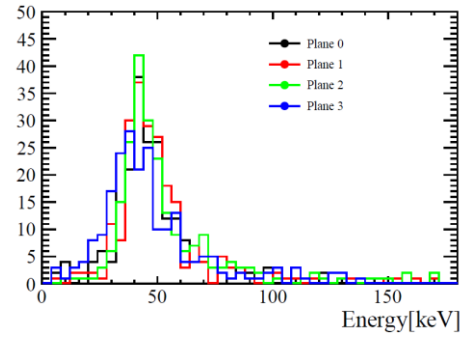


Figure 5: Atmospheric muons energy deposition on each plane.

## 6. CONCLUSION

Using a proof-of-concept prototype it was possible to reconstruct trajectories of atmospheric muons with spatial resolutions of 20  $\mu\text{m}$ , which can still be reduced by alignment improvements. The full COMBAT setup will use 8 detector planes, increasing the tracking quality and resolution.

## REFERENCES

- [1] LHCb collaboration, A. A. Alves Jr. et al., The LHCb detector at the LHC, JINST 3 (2008) S08005.
- [2] Particle Data Group, J.J Beatty, J. Matthews, T.K Gaisser, T.Stanev, "Review of Particle Physics", Phys. Rev.D86(2012), p.305-311.
- [3] Particle Data Group, H.Bichsel, D.E.Groom, S.R.Klein, "Review of Particle Physics", Phys. Rev.D86(2012), p. 323-338.
- [4] X. Llopert et.al. Timepix, a 65k programmable pixel readout chip. NIM A, 581:485–494,
- [5] S. Pospsil J. Uher D. Vavrk Z. Vykydal T. Holy, J. Jakubek. Data acquisition and processing software package for Medipix-2 device. NIM A, 563:254–258, 2006
- [6] J. Visser et al., "A Gigabit per Second Read-Out System for Medipix Quads", NIM A Vol 633, pages S22-S25, 2011

[6] J. Visser et al., “A Gigabit per Second Read-Out System for Medipix Quads”, NIM A Vol 633, pages S22-S25, 2011.